한국정밀공학회지 제 43 권 제 8 호 pp. 871-879
August 2026 / 871
J. Korean Soc. Precis. Eng., Vol. 43, No. 8, pp. 871-879
http://doi.org/10.7736/JKSPE.026.00025
ISSN 1225-9071 (Print) / 2287-8769 (Online)

PDMS 기반 방진 장갑의 손-팔 진동 전달률 비교에 관한 연구

Comparison of Hand-arm Vibration Transmissibility of PDMS-based Anti-vibration Gloves

이거성[1], 이민형[1], 이길용[1,2,#]
Geo-Sung Lee[1], Min-Hyeong Lee[1], and Gil-Yong Lee[1,2,#]

1 국립금오공과대학교 대학원 항공기계전자융합전공 (Department of Aeronautics, Mechanical and Electronic Convergence Engineering, Graduate School, Kumoh National Institute of Technology)
2 국립금오공과대학교 기계공학부 (Department of Mechanical Engineering, Kumoh National Institute of Technology)
Corresponding Author / E-mail: gylee@kumoh.ac.kr, TEL: +82-54-478-7293
ORCID: 0000-0002-9507-746X

KEYWORDS: Soft foam (소프트 폼), Anti-vibration glove (방진 장갑), Hand-arm vibration (손-팔 진동), Vibration transmissibility (진동 전달률)

Hand-arm vibration exposure is a recognized occupational hazard that can cause discomfort and long-term disorders. While anti-vibration gloves are commonly used to reduce these effects, their effectiveness is often limited by the stiffness of the materials and structural constraints. This study focuses on the development and evaluation of polydimethylsiloxane (PDMS)-based anti-vibration layers with varying internal structures for use in anti-vibration gloves. We prepared three types of PDMS layers: solid PDMS without pores (SPDMS), porous PDMS foam created through a sugar-leaching process (FPDMS), and a hybrid PDMS structure that combines solid and porous layers (HPDMS), all shaped like palms. These PDMS layers were integrated into glove specimens, and their vibration transmissibility was assessed using a measurement system compliant with ISO 10819:2013. Vibration transmissibility was recorded across one-third octave bands from 25 to 1,250 Hz, and frequency-weighted transmissibility values were calculated for both the M- and H-spectra. The results indicate that PDMS-based anti-vibration layers with controlled porosity can be effectively fabricated and incorporated into glove structures, and that variations in internal porosity significantly impact the measured vibration transmissibility characteristics.

Manuscript received: March 9, 2026 / Revised: May 18, 2026 / Accepted: May 20, 2026

1. Introduction

Hand-arm vibration generated by powered tools is a documented cause of discomfort and chronic disorders such as vascular and neurological impairments associated with hand-arm vibration syndrome (HAVS) [1-6]. Workers in construction, manufacturing, and forestry routinely handle tools that produce broadband vibration, and prolonged exposure can lead to reduced work performance and long-term health risks. Anti-vibration gloves are commonly used as a measure to reduce these effects [4,7,8]. However, many existing products show limited attenuation within the frequency ranges relevant to occupational tasks, and improvements in damping performance often introduce practical drawbacks such as increased thickness, reduced flexibility, or compromised grip stability [5,8-10]. These issues indicate the need for material systems that can reduce vibration while maintaining comfort and usability. PDMS (polydimethylsiloxane) is a silicone elastomer with mechanical properties that can be adjusted by controlling the mixing ratio of resin and curing agent [11]. Its softness, stability, and processability have led to its use in various wearable and cushioning components. When a water-soluble porogen such as sugar is mixed into uncured PDMS and later dissolved after curing, pores remain within the polymer matrix. This sugar-leaching process decreases the effective stiffness of the material and introduces internal pores, thereby increasing the compliance of the PDMS layer under external loading. Such increased compliance can result in larger deformation of porous PDMS layers, which may affect vibration transmissibility during hand-arm vibration exposure [12-16]. However, the vibration transmissibility characteristics of PDMS layers with controlled porosity under hand-arm vibration conditions relevant to protective gloves remain insufficiently studied.

Here, we investigate the vibration transmissibility of PDMS layers prepared in three forms: solid PDMS without pores (SPDMS), porous PDMS foam fabricated by sugar leaching (FPDMS), and a hybrid PDMS composed of solid and porous layers (HPDMS). These layers were fabricated in palm-shaped geometries for glove integration, and the effect of internal porosity on vibration transmissibility was examined. To evaluate their vibration transmissibility, the fabricated PDMS layers were incorporated into glove specimens and tested using a measurement system. A band-limited random vibration covering the one-third octave bands from 25 to 1,250 Hz was applied, and acceleration responses measured at the handle and the palm adapter were used to determine the vibration transmissibility. The measured signals were analyzed in one-third octave bands, and frequency-weighted transmissibility values were obtained using the weighting functions defined for the M- and H-spectra. The results show how internal porosity influences vibration transmissibility.

The design objective of the PDMS-based glove specimens was to reduce the frequency-weighted vibration transmissibility while maintaining a palm-shaped structure that could be integrated into a glove. SPDMS was used as a non-porous baseline to examine the effect of PDMS mixing ratio. FPDMS was designed to increase structural compliance and internal deformation through sugar-leached pores, with the expectation of reducing vibration transmissibility. HPDMS was introduced to combine the compliance of the porous layer with the load-bearing function of the solid layer, thereby limiting excessive compression of the porous structure under grip force.

2. Materials and Methods

2.1 Materials Used for Glove Specimens

Cotton work gloves, polydimethylsiloxane (PDMS; Sylgard 184, Dow Corning) and its curing agent, and commercial sugar were used to fabricate the anti-vibration layers. Palm-shaped molds were designed based on the glove geometry and fabricated using a fused deposition modeling (FDM) 3D printer (F170, Stratasys). The PDMS resin–curing agent mixture was prepared by combining

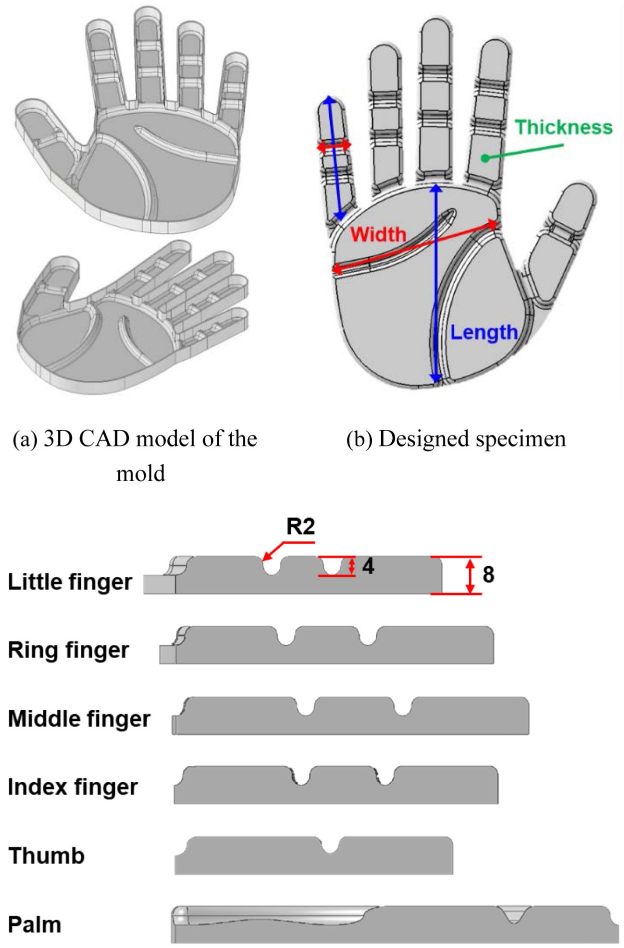

(a) 3D CAD model of the mold (b) Designed specimen

(c) Cross-sectional views of the palm and finger regions

Fig. 1 Geometric design of the PDMS-based anti-vibration glove specimen

PDMS resin and curing agent at mass ratios of 10 : 1, 20 : 1, and 30 : 1, stirring at 200 rpm for 1 hour until uniform, and degassing under vacuum. The PDMS-sugar mixture was prepared by combining PDMS resin, curing agent, and sugar, followed by stirring at 200 rpm for 1 hour and vacuum degassing. All mixtures were cured at 65°C for 3 hours.

2.2 Participants

The vibration experiments were performed by two male participants involved in the study. Both individuals were free from known upper-limb injuries and had no diagnosed neurological or musculoskeletal conditions affecting hand function. The experimental protocol was approved by the Institutional Review Board (IRB) Kumoh National Institute of Technology. Prior to the experiments, the investigators reviewed the experimental procedures and provided written informed consent. The values reported in Figs. 8-10 and Table 3 represent the mean values obtained from two participants, and the error bars indicate the

Table 1 Geometric dimensions, contact areas, and volumes of each region of the PDMS-based anti-vibration layer

	Thickness [mm]	Width [mm]	Length [mm]	Contact area [mm^2]	Volume [mm^3]
Palm	8	80	93.5	5,325	54,891
Thumb	8	20	60.5	680	8,681
Index finger	8	17	68.5	634	8,581
Middle finger	8	17	75.5	699	9,231
Ring finger	8	15.5	68	564	7,818
Little finger	8	15.5	57.5	404	6,208

standard deviation between the participant-averaged values. Because the number of participants was limited, the error bars should be interpreted as variability under the present laboratory conditions rather than as population-level statistical variation.

2.3 Geometric Design of PDMS-based Anti-vibration Gloves

The geometry of the PDMS-based anti-vibration glove specimen was designed in accordance with ISO 10819:2013. Fig. 1(a) shows the three-dimensional CAD model of the mold, and Fig. 1(b) presents the designed specimen with a thickness of 8 mm.

Cross-sectional views of the palm and finger regions are shown in Fig. 1(c). To allow finger flexion, 4 mm–deep slots were added to the knuckle and palm joint regions of the palm-shaped layer. The geometric dimensions, contact areas, and volumes of each region are summarized in Table 1. The dimensions were defined based on the geometry of the glove used in the experiments. The total volume of the anti-vibration layer was calculated from the CAD model to be approximately 104.95 cm^3.

3. Results and Discussion

3.1 Fabrication of PDMS-based Anti-vibration Gloves

Three types of anti-vibration layers were fabricated for glove integration: solid PDMS without pores (SPDMS), porous PDMS foam (FPDMS), and a hybrid PDMS composed of solid and porous layers (HPDMS). The fabrication processes for each structure are schematically illustrated in Fig. 2. As shown in Fig. 2(a), the SPDMS specimen was fabricated by casting the PDMS resin-curing agent mixture into a palm-shaped mold, followed by curing and demolding to obtain a dense, non-porous layer. Fig. 2(b) illustrates the fabrication of the FPDMS layer using a sugar-leaching process. A cured PDMS–sugar mixture was demolded and subsequently subjected to ultrasonic cleaning at 40 kHz and 60°C for 1 day to remove the sugar phase, resulting in the FPDMS

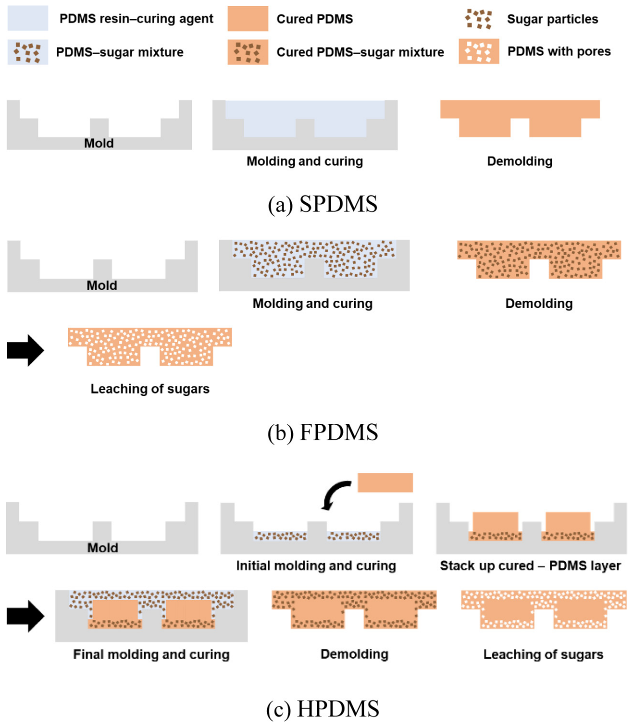

Fig. 2 Schematic illustration of the fabrication processes for PDMS-based anti-vibration layers

Table 2 Mass composition of the PDMS-based anti-vibration layer specimens, including SPDMS, FPDMS, and HPDMS

Specimen	Type	PDMS resin : curing agent : sugar mass ratio	PDMS resin [g]	Curing agent [g]	Sugar [g]
SPDMS10	Solid	10 : 1 : 0	89.34	8.93	0
SPDMS20		20 : 1 : 0	93.59	4.68	0
SPDMS30		30 : 1 : 0	95.10	3.17	0
FPDMS10	Foam	10 : 1 : 16.87	44.67	4.47	75.37
FPDMS20		20 : 1 : 32.21	46.80	2.34	75.37
FPDMS30		30 : 1 : 47.55	47.55	1.59	75.37
HPDMS30	Solid	30 : 1 : 0	30.00	1.00	0
	Foam	30 : 1 : 47.55	32.55	1.08	51.59

specimen. The fabrication process of the HPDMS layer is shown in Fig. 2(c). An initial porous layer with a thickness of 2 mm was formed from a PDMS–sugar mixture. A solid PDMS layer with a thickness of 4 mm was then placed on top of the porous layer, and the remaining volume was filled with a PDMS–sugar mixture. After curing and demolding, the specimen underwent the same sugar-leaching process to obtain the HPDMS specimen.

Table 2 summarizes the fabrication details of the SPDMS, FPDMS, and HPDMS specimens. For SPDMS and FPDMS, PDMS resin and curing agent were mixed at mass ratios of 10 : 1,

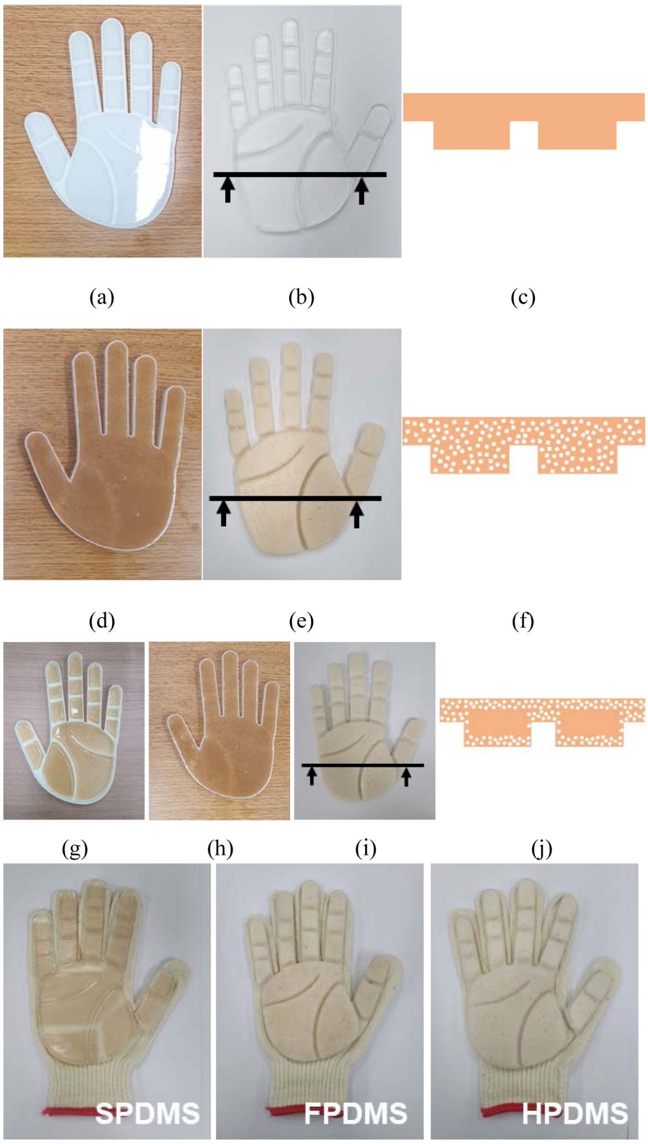

Fig. 3 Fabrication process of PDMS-based anti-vibration glove specimens: (a) molded SPDMS layer, (b) cured specimen, (c) cross-sectional schematic of SPDMS, (d) molded FPDMS before sugar removal, (e) specimen after demolding and leaching, (f) cross-sectional schematic of FPDMS, (g) placement of a solid layer onto a porous layer, (h) stacked HPDMS structure, (i) completed specimen after demolding, (j) cross-sectional schematic of HPDMS, and (k) completed glove specimens

20 : 1, and 30 : 1. Based on the densities of PDMS (r = 1.03 g/cm^3) and sugar (r = 1.58 g/cm^3), the amount of sugar was adjusted to obtain a foam density of approximately 50% in the FPDMS specimens. The HPDMS specimen was fabricated by combining a solid PDMS layer prepared at a mass ratio of 30 : 1 with a porous PDMS foam layer having a foam density of approximately 50%. The detailed masses of PDMS resin, curing agent, and sugar used for each specimen are listed in Table 2.

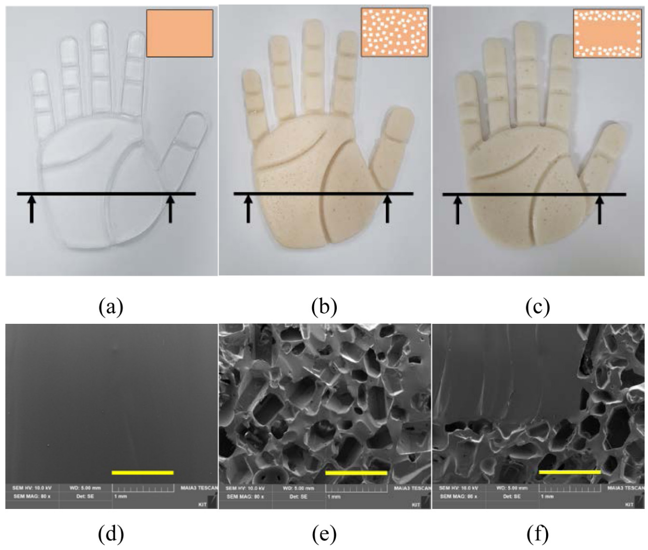

Fig. 4 PDMS-based anti-vibration specimens with cross-sectional schematics for (a) SPDMS, (b) FPDMS, and (c) HPDMS. SEM images of the cross sections of (d) SPDMS, (e) FPDMS, and (f) HPDMS. Scale bars are 1 mm in (d)-(f)

Fig. 3 illustrates the fabrication sequence and final configurations of the PDMS-based anti-vibration glove specimens. Figs. 3(a) and 3(b) show the molded and cured SPDMS layer and the corresponding palm-shaped specimen, with its cross-sectional structure schematically illustrated in Fig. 3(c).

Figs. 3(d) and 3(e) show the molded FPDMS specimen before sugar removal and the porous FPDMS specimen obtained after demolding and sugar leaching, respectively; the corresponding cross-sectional structure is shown in Fig. 3(f). Figs. 3(g)-3(i) show the HPDMS specimen during layer stacking, including the placement of a solid PDMS layer on a preformed porous layer and the completed specimen after curing and demolding; the corresponding cross-sectional schematic is provided in Fig. 3(j). Each PDMS layer was attached to a cotton work glove using fabric tape (108FR, Polyken, USA), and representative images of the completed glove specimens are shown in Fig. 3(k). Figs. 3(a), 3(d), 3(g), and 3(h) were taken while the resin was still placed in the mold, where the bottom side of the mold corresponded to the palm side of the glove specimen. The other specimen images in Fig. 3 were taken from the palm side after demolding.

3.2 Observations of Microstructures of Anti-vibration Layers with Different PDMS Types

To examine the porous morphology of the fabricated anti-vibration layers and the interfacial condition of the layered structure, the microstructures of SPDMS, FPDMS, and HPDMS were observed. Figs. 4(a)-4(c) present the specimens of SPDMS,

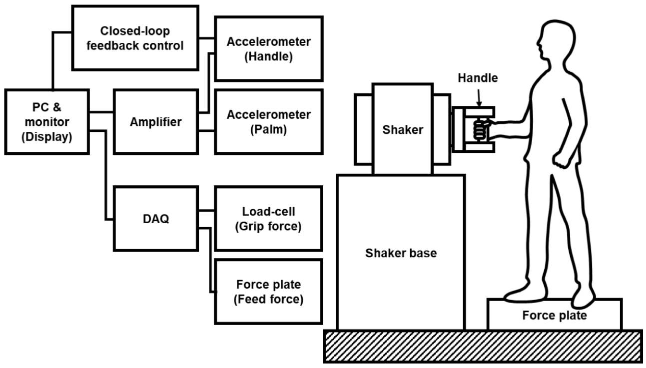

Fig. 5 Schematic diagram of the hand-arm vibration transmissibility evaluation system for anti-vibration gloves

FPDMS, and HPDMS, with inset schematics indicating the corresponding cross-sectional structures. Figs. 4(d)-4(f) show scanning electron microscopy (SEM) images of the cross sections of SPDMS, FPDMS, and HPDMS, respectively.

SPDMS exhibits a dense, non-porous morphology, whereas FPDMS shows a porous internal structure, with pores below approximately 0.5 mm in size distributed throughout the material, as shown in Fig. 4(e). In the HPDMS specimen, similar pore features are observed in the foam layer together with a continuous interface between the solid and porous layers, with no apparent interfacial defects or delamination, as shown in Fig. 4(f).

3.3 Evaluation of Hand-arm Vibration Transmissibility of the PDMS-based Anti-vibration Glove Specimens

Fig. 5 shows a schematic diagram of the hand-arm vibration transmissibility evaluation system built in accordance with ISO 10819:2013 [17]. The vibration experiments were conducted in one-third octave bands covering the frequency range from 25 to 1,250 Hz. The M-spectrum corresponds to the frequency range from 25 to 200 Hz, while the H-spectrum spans from 200 to 1,250 Hz. Vibration transmissibility was calculated as the ratio of the one-third octave band acceleration measured at the palm adapter to that measured at the handle [5,7-10]. A grip force of 30 ± 5 N and a feed force of 50 ± 8 N were maintained and monitored in accordance with the ISO requirements [6,17,18]. For measurements performed using only the palm adapter without an anti-vibration glove, the vibration transmissibility was required to remain within the range of 0.95 to 1.05 of unity under a contact force of 80 ± 10 N.

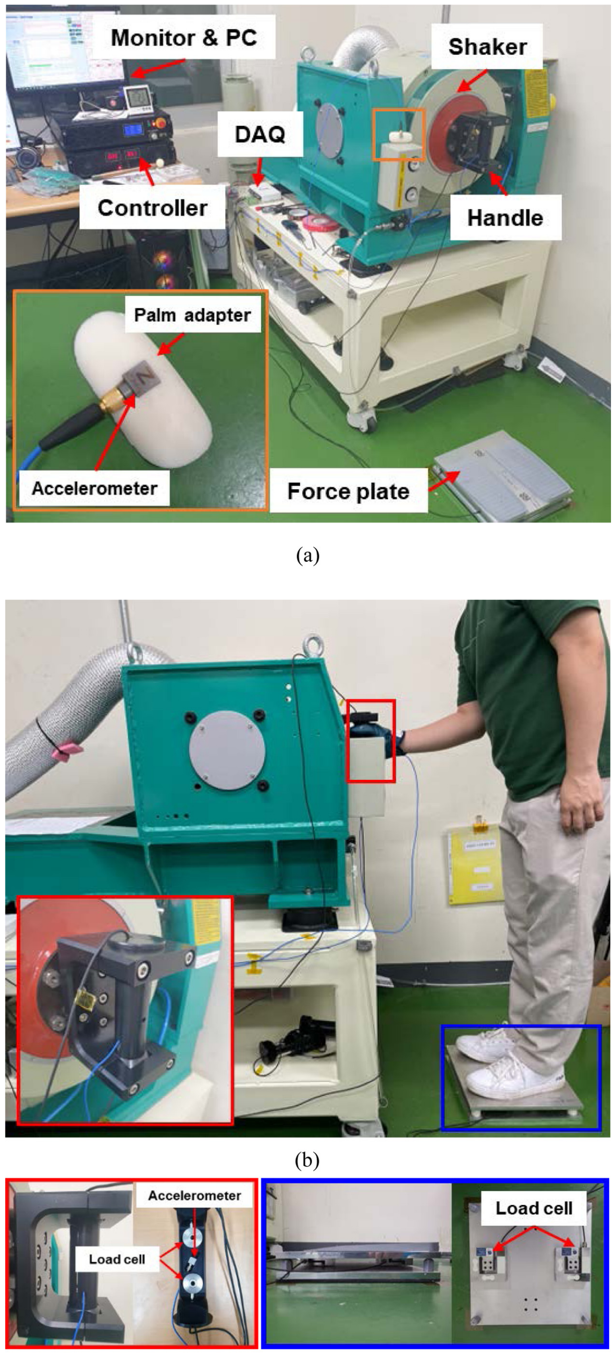

(a) (b) (c) (d)

Fig. 6 Experimental setup of the hand-arm vibration transmissibility evaluation system: (a) overall configuration of the experimental setup, (b) hand-arm vibration and force measurement configuration, consisting of (c) the handle and (d) the force plate

Fig. 6 presents the experimental setup corresponding to the schematic shown in Fig. 5. Fig. 6(a) shows the overall configuration of the hand-arm vibration transmissibility evaluation system, including the electrodynamic shaker (JINN, Korea), a handle with a diameter of 40 mm, a palm adapter, and force measurement components. The palm adapter incorporated an accelerometer (356A33, PCB Piezotronics, USA) to measure the vibration transmitted to the palm during the experiments. As shown in Fig. 6(b), the subject wore the glove specimen together with the palm adapter while vibration was applied through the handle. The vibration input was feedback-controlled using the acceleration signal measured by an accelerometer embedded inside the handle (333B30, PCB Piezotronics, USA), as shown in Fig. 6(c). The acceleration responses measured at the handle and the palm adapter were analyzed in one-third octave bands to determine vibration transmissibility. To compensate for the frequency response of the palm adapter, reference transmissibility values were obtained by measuring the vibration transmissibility with the palm adapter attached directly to the handle without an anti-vibration glove [7,8]. For the anti-vibration glove specimens, the measured vibration transmissibility was corrected using the reference transmissibility. The corrected transmissibility values were then frequency-weighted using the weighting coefficients specified for the M- and H-spectra [17]. In accordance with ISO 10819:2013 [17], the mean values of the frequency-weighted corrected vibration transmissibility, denoted as T_M and T_H, were calculated over the one-third-octave bands within the M-spectrum (25–200 Hz) and the H-spectrum (200–1,250 Hz), respectively, as shown in Eqs. (1)-(2) [17].

$$T_i = \frac{a_{palm,i}}{a_{handle,i}} \tag{1}$$

where, $a_{palm,i}$ and $a_{handle,i}$ are palm adapter and handle accelerations, respectively, measured at each frequency f_i.

$$T_M = \frac{\sum_{i\in M} w_i T_i}{\sum_{i\in M} w_i} \quad \text{and} \quad T_H = \frac{\sum_{i\in H} w_i T_i}{\sum_{i\in H} w_i} \tag{2}$$

The grip force was measured using an internal load cell (CWFS-20, BONGSHIN, Korea) integrated into the instrumented handle, as shown in Fig. 6(c).

The feed force was measured using a load cell (CMA9852-100, CASSCALE KOREA, Korea) integrated into the force plate on which the subject stood, as shown in Fig. 6(d). During the measurements, the subject stood upright, and the angle between the upper arm and the forearm was maintained at approximately 90°. Grip force and feed force were monitored in real time to ensure that the prescribed force conditions were maintained throughout the measurement.

After the vibration transmissibility measurements, the FPDMS specimens were visually inspected. No macroscopic fracture, tearing, or detachment from the glove was observed under the present test conditions. However, this observation only confirms the absence of visible damage after the laboratory transmissibility test and does not represent a quantitative durability assessment. Cyclic durability, fatigue resistance, and long-term wear behavior should be evaluated in future work.

Fig. 7 shows the vibration transmissibility measured using the palm adapter in direct contact with the handle, without an anti-vibration glove, under a contact force of 80 ± 10 N. The measured palm adapter transmissibility remained within the range of 0.95 to 1.05 across the one-third-octave bands from 25 to 1,250 Hz, satisfying the validity criterion specified in ISO 10819:2013 [17]. This result confirms that the measurement system met the required conditions for evaluating glove vibration transmissibility.

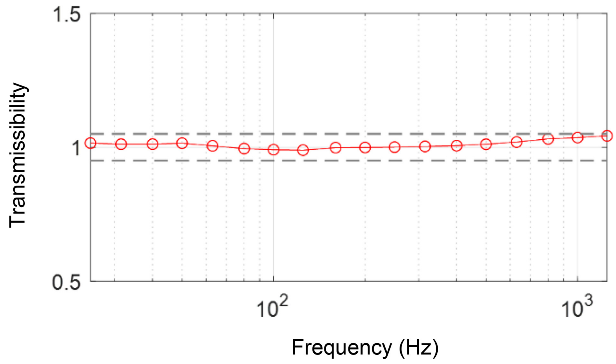

Fig. 7 Measured vibration transmissibility of the palm adapter without an anti-vibration glove

Figs. 8(a) and 8(b) show the corrected vibration transmissibility of two types of anti-vibration glove specimens, SPDMS and FPDMS, respectively, prepared with different PDMS resin-to-curing-agent ratios. In Fig. 8(a), the corrected vibration transmissibility of SPDMS decreased as the PDMS resin-to-curing-agent ratio increased. In contrast, Fig. 8(b) shows that the corrected vibration transmissibility of FPDMS increased with increasing PDMS resin-to-curing-agent ratio. Notably, for the FPDMS specimens, a pronounced increase in corrected vibration transmissibility was observed as the PDMS resin-to-curing-agent ratio increased from 20 : 1 to 30 : 1. As the PDMS resin-to-curing-agent ratio increased, the porous PDMS foam was likely compressed under the applied grip force, leading to reduced vibration attenuation. These results indicate that the vibration transmissibility of PDMS-based anti-vibration layers can be tailored by adjusting the PDMS resin-to-curing-agent ratio, and that the effect of this parameter differs between solid and porous PDMS structures. The opposite trends observed for SPDMS and FPDMS indicate that the effect of the resin-to-curing-agent ratio cannot be interpreted solely by the bulk stiffness of PDMS. In the non-porous SPDMS structure, an increase in the resin-to-curing-agent ratio is expected to reduce the crosslink density and effective stiffness, which can improve vibration isolation. In contrast, in the porous FPDMS structure, the reduced stiffness may promote compression and partial densification of the pore network under the prescribed grip and feed forces. This compression can decrease the effective pore volume and increase the number of load-bearing contact paths, thereby reducing the

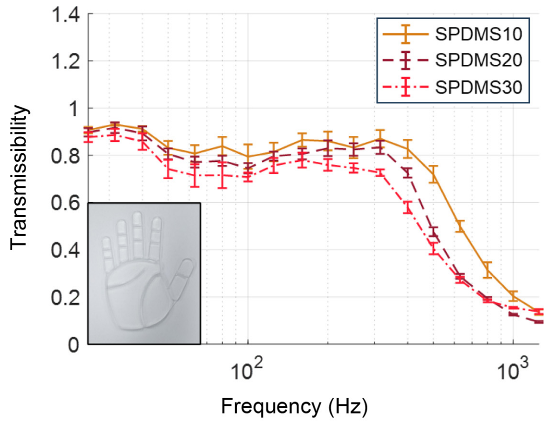

(a)

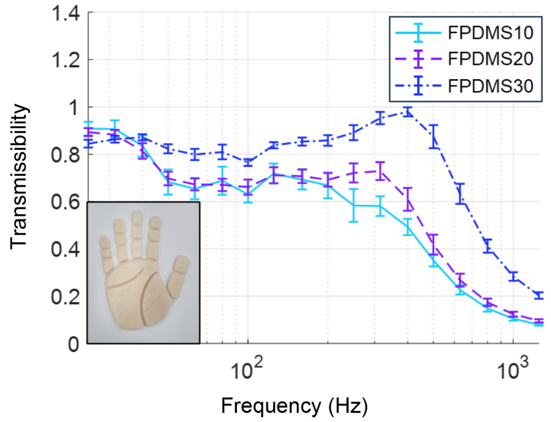

(b)

Fig. 8 Corrected vibration transmissibility of the anti-vibration glove specimens with (a) SPDMS and (b) FPDMS fabricated with different PDMS resin-to-curing-agent ratios

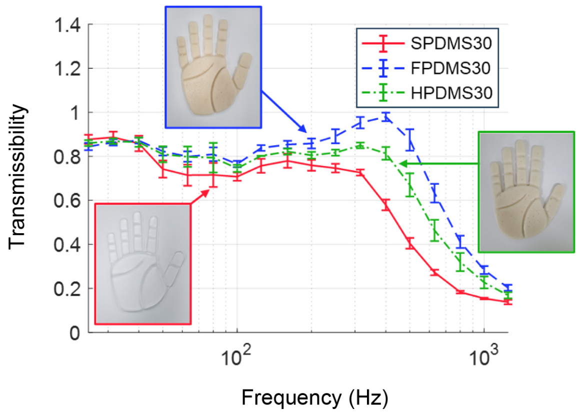

Fig. 9 Corrected vibration transmissibility of the anti-vibration glove specimen with HPDMS in comparison with SPDMS and FPDMS fabricated with a PDMS resin-to-curing-agent mass ratio of 30 : 1

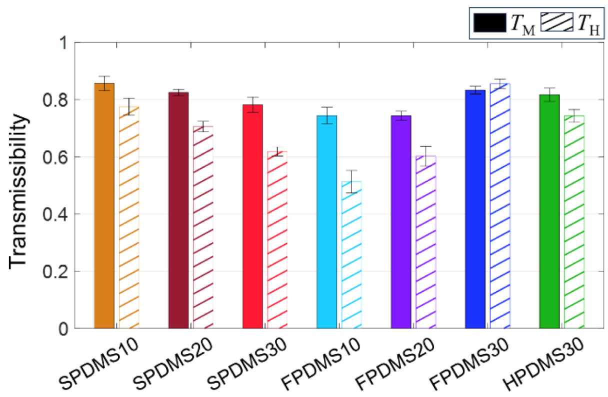

Fig. 10 Comparison of the frequency-weighted vibration transmissibility values (T_M and T_H) of the anti-vibration glove specimens in the M- and H-spectra

vibration attenuation effect, particularly in the H-spectrum where the response is more sensitive to local dynamic stiffness and contact conditions.

Fig. 9 shows the corrected vibration transmissibility of the HPDMS glove specimen in comparison with those of the SPDMS and FPDMS glove specimens. All specimens were fabricated using the same PDMS resin-to-curing-agent mass ratio of 30 : 1. As shown in Fig. 9, the vibration transmissibility of the HPDMS glove specimen is distributed between those of the SPDMS and FPDMS glove specimens over the measured frequency range. This behavior is attributed to the layered configuration of HPDMS, in which solid and foam PDMS layers are combined.

Compared with the FPDMS glove specimen, the HPDMS glove specimen exhibits lower vibration transmissibility due to the presence of the solid PDMS layer, which increases the effective stiffness under the applied grip force. In contrast, compared with the SPDMS glove specimen, the inclusion of the foam layer reduces the overall stiffness of the anti-vibration layer. As a result,

Table 3 Frequency-weighted vibration transmissibility values (T_M and T_H) of the anti-vibration glove specimens

Specimen	T_M	T_H
SPDMS10	0.857 ± 0.025	0.775 ± 0.030
SPDMS20	0.825 ± 0.011	0.706 ± 0.018
SPDMS30	0.782 ± 0.027	0.619 ± 0.016
FPDMS10	0.744 ± 0.029	0.513 ± 0.039
FPDMS20	0.744 ± 0.016	0.602 ± 0.035
FPDMS30	0.833 ± 0.014	0.855 ± 0.016
HPDMS30	0.817 ± 0.023	0.743 ± 0.023

the HPDMS glove specimen shows intermediate vibration transmissibility characteristics between the SPDMS and FPDMS glove specimens.

The frequency-weighted vibration transmissibility values in the M-spectrum (T_M) and H-spectrum (T_H) for each glove specimen are summarized in Table 3 and shown in Fig. 10.

For the SPDMS glove specimens, both T_M and T_H decreased as the PDMS resin-to-curing-agent ratio increased, which is attributed to the reduced stiffness of the solid PDMS layer at higher resin-to-curing-agent ratios. In contrast, the FPDMS glove specimens exhibited distinct behavior depending on the resin-to-curing-agent ratio. The FPDMS specimen fabricated at a ratio of 10 : 1 showed the lowest frequency-weighted transmissibility values among all tested specimens (T_M = 0.744 and T_H = 0.513), indicating the highest vibration attenuation performance among the fabricated specimens. As the resin-to-curing-agent ratio increased to 30 : 1, both T_M and T_H increased, indicating a reduction in vibration attenuation as the porous structure appears to be compressed under the applied grip force. The HPDMS glove specimen fabricated with a resin-to-curing-agent ratio of 30 : 1 showed T_M and T_H values that were higher than those of the corresponding SPDMS specimen and lower than those of the FPDMS specimen. This intermediate behavior reflects the combined structural response of the solid and porous layers, where the presence of the solid layer restricts excessive compression of the porous layer under the applied grip force. To investigate these effects, the influence of the porous layer on finger motion and deformation behavior under grip force will be examined in future studies.

Although direct measurements of compressive modulus and damping ratio were not performed in this study, the transmissibility results shown in Fig. 10 and Table 3 provide a quantitative comparison of the structure-dependent vibration response. For example, the FPDMS10 specimen showed the lowest values of T_M and T_H, whereas FPDMS30 showed markedly higher values, indicating that the vibration attenuation performance of the porous structure is strongly affected by the PDMS mixing ratio and deformation state under grip force.

4. Conclusion

In summary, this study investigated the vibration transmissibility characteristics of PDMS-based anti-vibration layers with different levels of internal porosity fabricated using a sugar-leaching process and applied to glove specimens. Solid PDMS without pores (SPDMS), porous PDMS foam (FPDMS), and a hybrid PDMS structure combining solid and porous layers (HPDMS) were systematically prepared in palm-shaped geometries and integrated into anti-vibration gloves. The vibration transmissibility of the fabricated glove specimens was evaluated using a measurement system in accordance with ISO 10819:2013. By varying the PDMS resin-to-curing-agent ratio and internal porosity, the vibration attenuation behavior of each structure was examined using frequency-weighted transmissibility values in the M- and H-spectra. The experimental results showed that internal porosity has a clear influence on vibration transmissibility. Among the fabricated specimens, the FPDMS glove with a resin-to-curing-agent ratio of 10 : 1 exhibited the lowest frequency-weighted transmissibility values, indicating the highest vibration attenuation performance. In contrast, FPDMS specimens with higher resin-to-curing-agent ratios showed increased transmissibility, whereas SPDMS specimens exhibited improved attenuation with increasing resin-to-curing-agent ratio. The HPDMS specimen demonstrated intermediate vibration transmissibility characteristics between those of the SPDMS and FPDMS specimens, reflecting the combined response of solid and porous layers.

Although this study evaluated vibration transmissibility of PDMS-based glove specimens, detailed assessments of finger motion, and deformation behavior distribution under grip force were not included. Consequently, the mechanical response associated with internal porosity under grip force was not directly quantified. Nevertheless, the results confirm that porous PDMS structures with controlled internal porosity can be fabricated and incorporated into anti-vibration glove configurations, and that internal porosity plays an important role in determining vibration transmissibility. Overall, the findings of this study demonstrate the feasibility of using PDMS-based porous structures for anti-vibration glove applications and highlight the importance of controlling internal porosity to tailor vibration attenuation performance. Future work will focus on investigating the mechanical response of porous layers under grip force, including deformation behavior and finger motion, to further clarify the relationship between internal porosity and vibration attenuation and to support the optimization of PDMS-based anti-vibration glove designs.

ACKNOWLEDGEMENT

This work was supported by the grant funded by Ministry of Trade, Industry and Energy (MOTIE, Korea) and the Korea Evaluation Institute of Industrial Technology (KEIT) (Nos. 20006388 and 20017462), the National Research Foundation of Korea (NRF) grant funded by the Korea government (MSIT) (RS-2024-00459127), the Brain Korea 21 FOUR Project (Department of Aeronautics, Mechanical and Electronic Convergence Engineering, Kumoh National Institute of Technology), and the regional innovation system & education (RISE)-(Specialized Industry Scale-up) program through the Gyeongbuk RISE Center, funded by the Ministry of Education (MOE) and the Gyeongsangbuk-do, Republic of Korea (2026-rise-15-105).

REFERENCES

1. Bovenzi, M., Ronchese, F., Larese Filon, F., Marchetti, E., Tirabasso, A., Massotti, C., Tarabini, M., (2025), The role of personal risk factors in the occurrence of the hand-arm vibration syndrome: a pooled analysis of individual data from Italian cross-sectional and cohort studies, International Archives of Occupational and Environmental Health, 98(8), 757-774.
2. Nilsson, T., Wahlström, J., Burström, L., (2017), Hand-arm vibration and the risk of vascular and neurological diseases: A systematic review and meta-analysis, PLOS One, 12(7), e0180795.
3. Griffin, M. J., (1997), Measurement, evaluation, and assessment of occupational exposures to hand-transmitted vibration, Occupational and Environmental Medicine, 54(2), 73-89.
4. Milosevic, M., McConville, K. M. V., (2012), Evaluation of protective gloves and working techniques for reducing hand-arm vibration exposure in the workplace, Journal of Occupational Health, 54(3), 250-253.
5. Hewitt, S., Dong, R. G., Welcome, D. E., McDowell, T. W., (2015), Anti-vibration gloves?, Annals of Occupational Hygiene, 59(2), 127-141.
6. Dong, R. G., Wu, J. Z., McDowell, T. W., Welcome, D. E., Schopper, A. W., (2005), Distribution of mechanical impedance at the fingers and the palm of the human hand, Journal of Biomechanics, 38(5), 1165-1175.
7. Dong, R. G., Rakheja, S., McDowell, T. W., Welcome, D. E., Wu, J. Z., Warren, C., Barkley, J., Washington, B., Schopper, A. W., (2005), A method for assessing the effectiveness of anti-vibration gloves using biodynamic responses of the hand-arm system, Journal of Sound and Vibration, 282(3-5), 1101-1118.
8. Dong, R. G., Rakheja, S., Smutz, W. P., Schopper, A., Welcome, D., Wu, J. Z., (2002), Effectiveness of a new method (TEAT) to assess vibration transmissibility of gloves, International Journal of Industrial Ergonomics, 30(1), 33-48.
9. Griffin, M. J., (1998), Evaluating the effectiveness of gloves in reducing the hazards of hand-transmitted vibration, Occupational and Environmental Medicine, 55(5), 340-348.
10. Dong, R. G., Welcome, D. E., Peterson, D. R., Xu, X. S., McDowell, T. W., Warren, C., Asaki, T., Kudernatsch, S., Brammer, A., (2014), Tool-specific performance of vibration-reducing gloves for attenuating palm-transmitted vibrations in three orthogonal directions, International Journal of Industrial Ergonomics, 44(6), 827-839.
11. Sales, F. C. P., Ariati, R. M., Noronha, V. T., Ribeiro, J. E., (2022), Mechanical characterization of PDMS with different mixing ratios, Procedia Structural Integrity, 37, 383-388.
12. Cha, K. J., Kim, D. S., (2011), A portable pressure pump for microfluidic lab-on-a-chip systems using a porous polydimethylsiloxane (PDMS) sponge, Biomedical Microdevices, 13(5), 877-883.
13. Yin, J., Zhang, J., Zhang, Y., Wang, W., (2017), Porosity, mechanical properties, and damping ratio of particulate-filled polymer composite for precision machine tools, Journal of Applied Polymer Science, 134(6), 44435.
14. Si, J., Cui, Z., Xie, P., Song, L., Wang, Q., Liu, Q., Liu, C., (2016), Characterization of 3D elastic porous polydimethylsiloxane (PDMS) cell scaffolds fabricated by VARTM and particle leaching, Journal of Applied Polymer Science, 133(4), 42909.
15. Day, G. J., Zhang, Q., Remillat, C. D. L., Comandini, G., Perriman, A. W., Scarpa, F., (2025), Tunable network architecture in a hydrogel with extreme vibration damping properties, Communications Materials, 6(1), 148.
16. Lee, G.-S., Lee, S.-H., Lee, G.-Y., (2023), Tunable mechanical properties of Vectran liquid crystal polymer (LCP) short fiber-reinforced soft composite, Fibers and Polymers, 24(1), 207-220.
17. ISO 10819, (2013), Mechanical vibration and shock — Hand-arm vibration — Measurement and evaluation of the vibration transmissibility of gloves at the palm of the hand.
18. Dong, R. G., Welcome, D. E., Xu, X. S., Warren, C., McDowell, T. W., Wu, J. Z., Rakheja, S., (2012), Mechanical impedances distributed at the fingers and palm of the human hand in three orthogonal directions, Journal of Sound and Vibration, 331(5), 1191-1206.

Geo-Sung Lee
Received his M.S. degree in 2022 from Department of Mechanical Engineering, Kumoh National Institute of Technology. His research interests are additive manufacturing and vibration.
E-mail: rjtjd493@naver.com

Min-Hyeong Lee
Received his M.S. degree in 2026 from Department of Mechanical Engineering, Kumoh National Institute of Technology. His research interests are additive manufacturing and vibration.
E-mail: 20246060@kumoh.ac.kr

Gil-Yong Lee
Associate Professor in the Department of Mechanical Engineering, Kumoh National Institute of Technology. His research interests are integrated manufacturing system, sensors/actuators, composites, vibration, control, and additive manufacturing.
E-mail: gylee@kumoh.ac.kr